

Stearyl methacrylate co-polymers: towards new polymer coatings for mortars protection

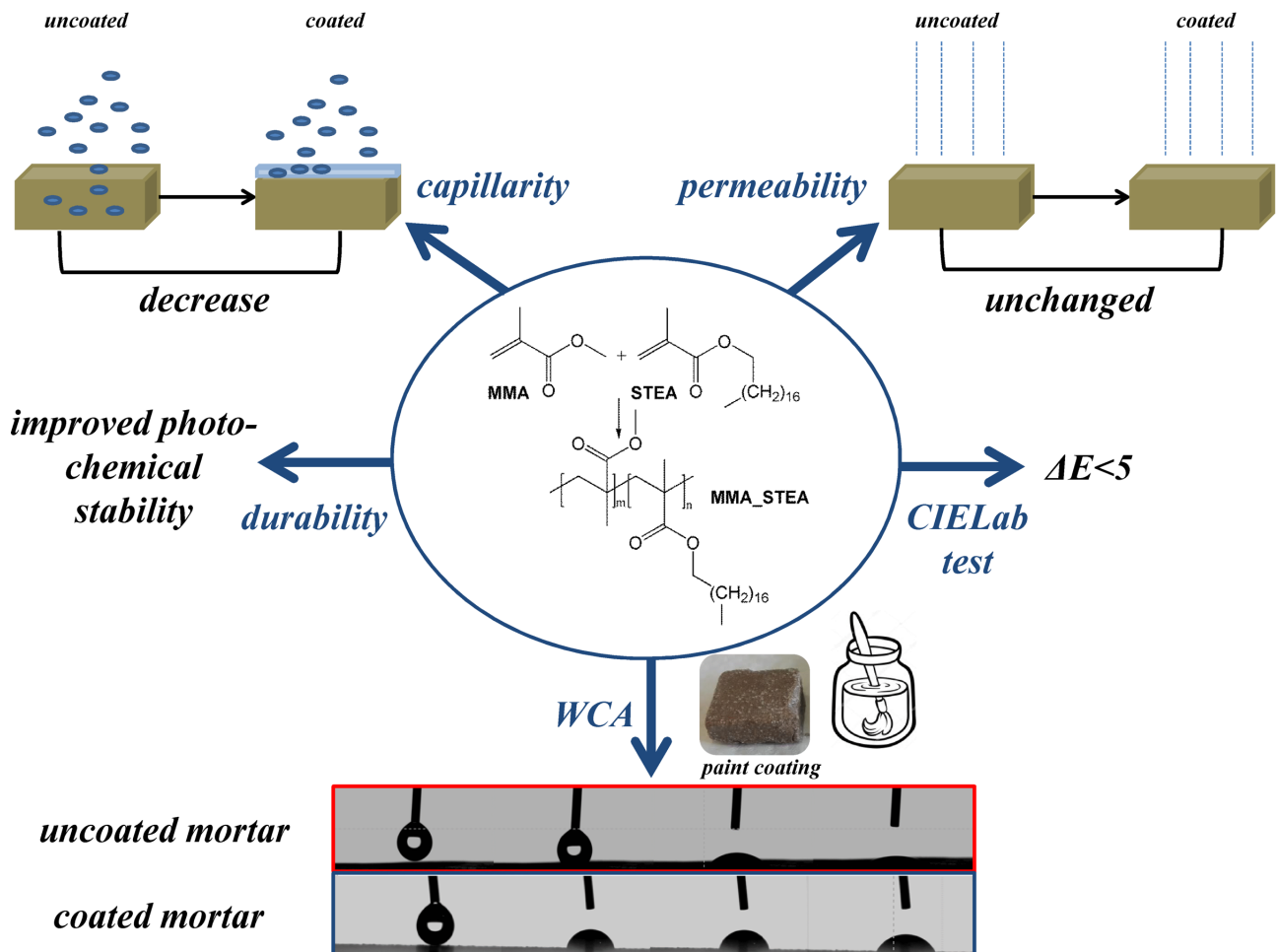
Valentina Sabatini^{a,b,c,*}, Eleonora Pargoletti^{a,b}, Martina Longoni^a, Hermes Farina^{a,b,c}, Marco Aldo Ortenzi^{a,b,c} and Giuseppe Cappelletti^{a,b,c,*}

^aDepartment of Chemistry, Università degli Studi di Milano, Via Golgi 19, 20133 Milan, Italy.

^bCRC Materials & Polymers Laboratory (LaMPo), Department of Chemistry, Università degli Studi di Milano, Via Golgi 19, 20133 Milan, Italy.

^cConsorzio Interuniversitario per la Scienza e Tecnologia dei Materiali (INSTM), Via Giusti 9, 50121, Firenze, Italy.

*Corresponding Authors; Phone: +39 02 503 14228, e-mail: giuseppe.cappelletti@unimi.it, valentina.sabatini@unimi.it



18 **ABSTRACT**

19 In the present work, a novel polymeric coating for mortars protection was prepared via free radical
20 polymerization between methyl methacrylate (MMA) and stearyl methacrylate (STEA) to overcome
21 the well-known technical problems related to the use of commercial Polyacrylic protectives. The
22 physico-chemical properties of MMA_STEA and the effect of different STEA amounts (1.0-2.5-
23 5.0% mol/mol respect to MMA) on MMA_STEA features were determined via ¹H NMR and FT-IR
24 spectroscopy, Gel Permeation Chromatography (GPC) and Differential Scanning Calorimetry
25 (DSC). Furthermore, the long-term behavior of these polymeric protective agents was evaluated by
26 means of accelerated aging tests exploiting UV radiations. MMA_STEA coatings were applied to
27 air-hardening calcic lime mortars and their performances were studied using different surface
28 techniques: static water contact angles (WCAs), CIELab colorimetric tests, water absorption by
29 capillarity and water vapor permeability (WVP). All measurements were also performed after an
30 UV aging test to study the durability of the coatings applied on mortar. This work demonstrates that
31 a polymer coating prepared starting from methyl and stearyl methacrylates-based comonomers is an
32 efficient way to obtain mortar protectives with satisfactory water repellent behavior, transparency
33 and durability.

34

35 *Keywords: cultural heritage, mortar, polymeric coating, free radical polymerization, surface*
36 *modification.*

37

38 **1. INTRODUCTION**

39 The protection of building materials, such as mortars, stones and marbles, is one of the most critical
40 and important steps for the conservation of cultural heritages and modern architectures.

41 The main causes of building materials deterioration exposed to outdoor conditions are water
42 permeation into the material [1], corrosion by chemical pollutants [2], freezing/thawing cycles [2]
43 and crystallization/precipitation of salts solutions absorbed from the environment [3].

44 Thus, the use of protective and consolidating coatings to construction materials is an efficient way
45 to hinder and protect cultural heritages and buildings from the natural decay, avoiding or limiting
46 the water penetration into the substrates [4,5].

47 A protective coating for a building material should satisfy several requirements: *i*) water repellency
48 reducing the capillarity rise, *ii*) minimum alteration of the natural water vapor permeability of the
49 material, *iii*) no significant variation of the aesthetical appearance, *iv*) durability against external
50 conditions and *v*) easiness of application and removal [6].

51 Up to now, two main categories of protectives for building materials are commercially available,
52 *i.e.* pure organic resins (such as polysiloxanes [7] and polyacrylates [8]), or hybrid coatings (TiO₂ or
53 SiO₂ together with polymers) [4]. Referring to organic products, polymer coatings prepared starting
54 from acrylic monomers are typically employed as protective agents of building materials for
55 cultural heritages and modern architectures [9]. During the last decades, the most satisfactory
56 commercial acrylic resin, (obtainable via free radical polymerization technique starting from a
57 mixture of acrylic and methacrylic monomers, ethyl methacrylate, EMA and methyl acrylate, MA),
58 was Paraloid B72[®], due to its good water repellence and optically clear appearance [10]. Despite the
59 common use of photo-stabilizing agents with Paraloid B72[®] [11], the presence in the acrylic
60 monomer of a hydrogen atom in alpha position to carbonyl group, that is capable to start photo-
61 chemical degradation reactions leads to severe durability issues [12].

62 To overcome the above-mentioned limits, in our previous works [13,14] we have exploited the use
63 of innovative polymer coatings as protectives of precious marbles showing satisfactory water
64 repellent properties and improved durability, combining the use of fluorinated and methacrylic
65 monomers and without the addition of any photo stabilizer agent.

66 Thus, the development of new polymer coatings able to overcome the technical problems
67 previously reported not only for precious stones but also for commercial marbles and mortars is still
68 a challenge. Despite fluorine-based coatings are considered the most promising candidates [15],
69 there are needs to work out the large-scale low-cost fabrication routes.

70 Hence, in order to overcome the above-mentioned limits of polyacrylic and polymethylmethacrylate
71 resins, the aim of the present work was to synthesize a new polymer coating combining the use of
72 methyl and stearyl methacrylates comonomers, without the addition of any fluorinated comonomer.
73 The effects in terms of water repellency of long alkyl chains on the surface properties of the
74 resulting coating have been deeply studied.

75 Specifically, a new type of polymer protective was prepared via free radical polymerization
76 between methyl methacrylate -MMA- and stearyl methacrylate -STEA- (MMA_STEA), changing
77 the loading of STEA comonomer (1.0-2.5-5.0% mol/mol respect to MMA). In order to determine
78 the long-term properties of MMA_STEA resins, accelerated exposure tests under UV radiations
79 were performed. The macromolecular structure, molecular weights and thermal features of
80 MMA_STEA resins, were investigated before and after the UV exposure simulation test via ¹H
81 NMR and Fourier Transform-Infrared (FT-IR) spectroscopies, Gel Permeation Chromatography
82 (GPC) and Differential Scanning Calorimetry (DSC) measurements.

83 Finally, the synthesized resins were applied on typical air-hardening calcic lime mortars and their
84 performances as protective agents were studied using different surface techniques such as water

85 contact angle measurements (WCA), CIELaB colorimetric analyses, water absorption by capillarity
86 and water vapor permeability (WVP). Furthermore, WCA, colorimetric, permeability and WVP
87 data were measured and compared before and after the accelerated ageing test.

88

89 **2. EXPERIMENTAL**

90 **2.1. Materials**

91 Methyl methacrylate (MMA, 99%), stearyl methacrylate (STEA, mixture of stearyl and cetyl
92 methacrylates), α,α' -Azobisisobutyronitrile (AIBN, 99%), toluene (99.8% anhydrous), methanol
93 (99.8% anhydrous), tetrahydrofuran (THF, 99.8% anhydrous), dichloromethane (DCM, 99.8%
94 anhydrous), distilled water Chromasolv[®] ($\geq 99.9\%$) and chloroform-d (CDCl_3 , 99.96 atom % D)
95 were supplied by Sigma Aldrich and used without purification. For the mortars preparation, white
96 cement (Portland cement, TECNOCEM, Italcementi S.p.A.), hydrated lime NHL 3.5 (from Soc.
97 Calce Raffinata, Savignano sul Panaro), pure quartz sand (0.1 – 0.3 mm, from C.T.S., Altavilla
98 Vicentina), GEO coarse pumice, fine pumice (Hess Pumice Idaho USA, 0.3 mm), thinner (Sika[®]
99 ViscoCrete[®] 5380, polystearic esters) and aerating agent (ARMIX, aqueous solution of sulfonated
100 polymers) were adopted.

101 **2.2 Synthesis of MMA_STEA copolymers**

102 Three MMA_STEA copolymers with increasing nominal amount of STEA -1.0_2.5_5.0% mol/mol-
103 respect to MMA comonomer were synthesized.

104 In a typical polymerization procedure, a 100 cm³ one-necked round bottom flask was equipped with
105 a nitrogen inlet adapter, a reflux condenser and an overhead magnetic stirrer. The flask was flushed
106 with nitrogen, charged with 40 cm³ of toluene, MMA, STEA and AIBN, the latter used as free
107 radical initiator at 1% mol/mol respect to MMA and STEA comonomers. The solution was put in an
108 oil bath, heated for 24 h at 80°C and then gradually cooled down to room temperature. The solution
109 obtained was precipitated into a large excess of methanol under stirring and a white solid precipitate
110 was obtained. The solid was recovered via filtration and washed at room temperature with distilled
111 water for several days under stirring to assure the complete removal of unreacted methacrylic
112 monomers from MMA_STEA samples. After washing, the polymers were dried in a vacuum oven
113 (about 4 mbar) at 40°C for 48 h and then the absence of residual solvents was checked via
114 isothermal thermogravimetric analysis (TGA), performed for 2 h at 70°C under nitrogen flow.
115 Figure 1 shows the representative procedure for the synthesis of MMA_STEA co-polymers.

116

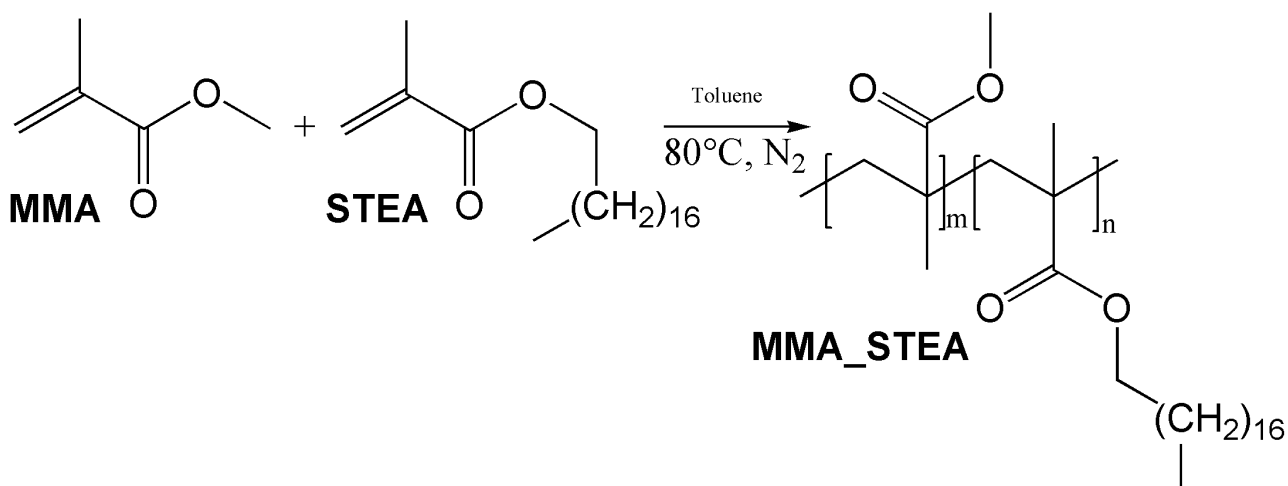


Figure 1. Synthetic route MMA_STEA copolymers.

117
118
119

120 2.3 Characterization of polymers

121 2.3.1 Nuclear magnetic resonance: ^1H NMR

122 ^1H NMR spectra were collected at 25°C with a BRUKER 400 MHz spectrometer. Samples for the
123 analyses were prepared dissolving 10-15 mg of MMA_STEA samples in 1 cm^3 of CDCl_3 .

124 2.3.2 UV exposure simulation test

125 To evaluate the stability of the polymers under UV radiations, an accelerated aging test was
126 performed according to UNI 10925:2001 standard method [16]. The test was conducted for 100 h
127 ($T = 25^\circ\text{C}$ and $p = 1\text{ atm}$), with Ultra Vitalux lamp characterized by a wavelength of 315-400 nm
128 for UVA rays and 280-315 nm for UVB ones.

129 2.3.3 Fourier Transform- Infrared (FT-IR)

130 FT-IR spectra of MMA_STEA polymers were obtained on a Spectrum 100 spectrophotometer
131 (Perkin Elmer) in attenuated total reflection (ATR) mode using a resolution of 4.0 and 256 scans, in
132 a range of wavenumber between 4000 and 400 cm^{-1} . A single-bounce diamond crystal was used
133 with an incidence angle of 45° . FT-IR spectra were collected before and after the UV aging test.

134 2.3.4 Differential Scanning Calorimetry (DSC)

135 DSC analyses were conducted using a Mettler Toledo DSC1; the samples were prepared weighting
136 from 5 to 10 mg each in a standard $40\text{ }\mu\text{L}$ aluminium pan, with an empty $40\text{ }\mu\text{L}$ aluminium pan as
137 reference and using the following thermal program: *i*) $25\text{-}150^\circ\text{C}$ at $10^\circ\text{C}/\text{min}$; *ii*) 5 min at 150°C ;
138 *iii*) $150\text{-}25^\circ\text{C}$ at $10^\circ\text{C}/\text{min}$; *iv*) 5 min at 25°C and *v*) $25\text{-}170^\circ\text{C}$ at $10^\circ\text{C}/\text{min}$. The thermal behaviour
139 of the samples obtained after the UV exposure simulation test was studied with the same thermal
140 program.

141 2.3.5 Gel Permeation Chromatography (GPC)

142 The effect of UV exposure on the molecular weight of the polymeric samples was evaluated using a
143 GPC system having Waters 1515 Isocratic HPLC pump and a four Phenomenex Phenogel ($5 \times 10^3 \text{Å}$ - $5 \times 10^4 \text{Å}$ - $5 \times 10^5 \text{Å}$ - $5 \times 500 \text{Å}$) columns set with a RI detector Waters 2487 using a flow rate of 1
144 cm^3/min and 40 μl as injection volume. Samples were prepared dissolving 40 mg of polymer in 1
145 cm^3 of THF; before the analysis, the solution was filtered with 0.45 μm filters. Molecular weight
146 data were expressed in polystyrene (PS) equivalents. The calibration was built using monodispersed
147 PS standards having the following nominal peak molecular weight (Mp) and molecular weight
148 distribution (D): Mp = 1600000 Da ($D \leq 1.13$), Mp = 1150000 Da ($D \leq 1.09$), Mp = 900000 Da
149 ($D \leq 1.06$), Mp = 400000 Da ($D \leq 1.06$), Mp = 200000 Da ($D \leq 1.05$), Mp = 90000 Da ($D \leq 1.04$), Mp
150 = 50400 Da ($D = 1.03$), Mp = 30000 Da ($D = 1.06$), Mp = 17800 Da ($D = 1.03$), Mp = 9730 Da
151 ($D = 1.03$), Mp = 5460 Da ($D = 1.03$), Mp = 2032 Da ($D = 1.06$), Mp = 1241 Da ($D = 1.07$), Mp = 906
152 Da ($D = 1.12$), Mp = 478 Da ($D = 1.22$); Ethyl benzene (molecular weight = 106 g/mol). For all
153 analyses, 1,2-dichlorobenzene was used as internal reference. The molecular weights of the samples
154 obtained after the UV exposure test were also determined.

156 **2.4 Mortar preparation and characterization**

157 2.4.1 Mortar formulation

158 Four mortar tiles of $5 \times 5 \times 1$ cm and four of $2 \times 2 \times 1$ cm were prepared as following: white cement
159 (134.1 g, 26.8% w/w), lime (45.0 g, 9.0% w/w), sand (45.0 g, 9.0% w/w), coarse pumice (44.7 g,
160 8.9% w/w), fine pumice (143.7 g, 28.7% w/w), deionized water (84.3 g, 16.9% w/w), thinner (2.7 g,
161 0.5% w/w) and aerating agent (0.3 g, 0.1% w/w) were thoroughly mixed in a 500 cm^3 plastic
162 container. Then, the viscous paste was put in epoxy molds and dried for 4 weeks in air at room
163 temperature in order to favour the carbonation process.

164 2.4.2 Scanning Electron Microscopy – Energy Dispersive X-ray Spectroscopy (SEM - EDX)

165 Mortar tiles morphology and elementary composition were determined by SEM Hitachi TM-1000
166 equipped with an energy dispersive X-ray spectroscopy EDX Hitachi ED3000. The investigations
167 were performed with an acceleration voltage of 15 kV and 50 pA of current probe.

168 **2.5 Application of polymer coatings on mortars surface and their characterization**

169 2.5.1 MMA_STEA application on mortars surface

170 Polymers were dissolved in DCM using 20% w/w concentration. The application of coatings on
171 mortars surface was carried out using a brush with bristles made with Polyamide 6 in order to
172 obtain a homogeneous and thin polymer layer of 200 mg (determined by weighing) onto the mortar
173 surface. The coated mortar tiles were dried at 40°C for 1 h and then used for water contact angles
174 analyses (WCA), CIELab colorimetric measurements, water absorption by capillarity and water
175 vapour permeability (WVP) tests. To evaluate the polymer stability under UV radiations, an

176 accelerated aging test was performed as reported in paragraph 2.3.2 and WCA, CIELab, capillarity
177 and WVP analyses were also repeated on aged coated mortars.

178 2.5.2 Water Contact Angle (WCA) analyses

179 Surface wetting properties of the both pristine and coated mortar tiles were assessed by contact
180 angle measurements using a Krüss Easydrop Instrument. The contact angle values were obtained by
181 depositing a drop (5 μL) of distilled water. At least fifteen measurements were taken on each
182 sample to get reliable values, averaging the obtained results. The wetting properties of the coated
183 samples, obtained after the UV exposure, were also determined.

184 2.5.3 CIELab colorimetric measurements

185 Colorimetric measurements were performed to verify the colour modification of the protective films
186 after the UV aging test. The chromatic coordinates were calculated according to the Commission
187 Internationale d'Eclairage (CIELab method) [17], starting from diffusive reflectance spectra
188 acquired in the UV-Vis spectral range from 800 to 200 nm with a UV-Vis SHIMADZU
189 spectrophotometer model UV 2600 instrument. According to the literature, no significant variation
190 occurs when $\Delta E^* < 5$ [18].

191 2.5.4 Water absorption by capillarity

192 Capillary water absorption measurements were performed on bare and coated materials by the
193 gravimetric sorption technique, as described in the standard protocol UNI EN 15801 [19]. Total
194 amount of water absorbed by a material (Q_f), capillary absorption (CA) and relative capillarity
195 index (CI_{rel} , which give information about the resistance to capillary rise when prolonged contact
196 with water occurs) were determined, accordingly.

197 2.5.5 Water vapour permeability (WVP)

198 WVP analyses of bare and coated mortars were evaluated by means of the methodology described
199 in the standard protocol UNI 15803 [20]. Reduction in Water Vapour Permeability (RVP) was
200 calculated; according to the standard protocol, a polymer material cannot be used as protective for
201 mineral substrate if $RVP > 50\%$. WVP analyses were repeated on aged materials.

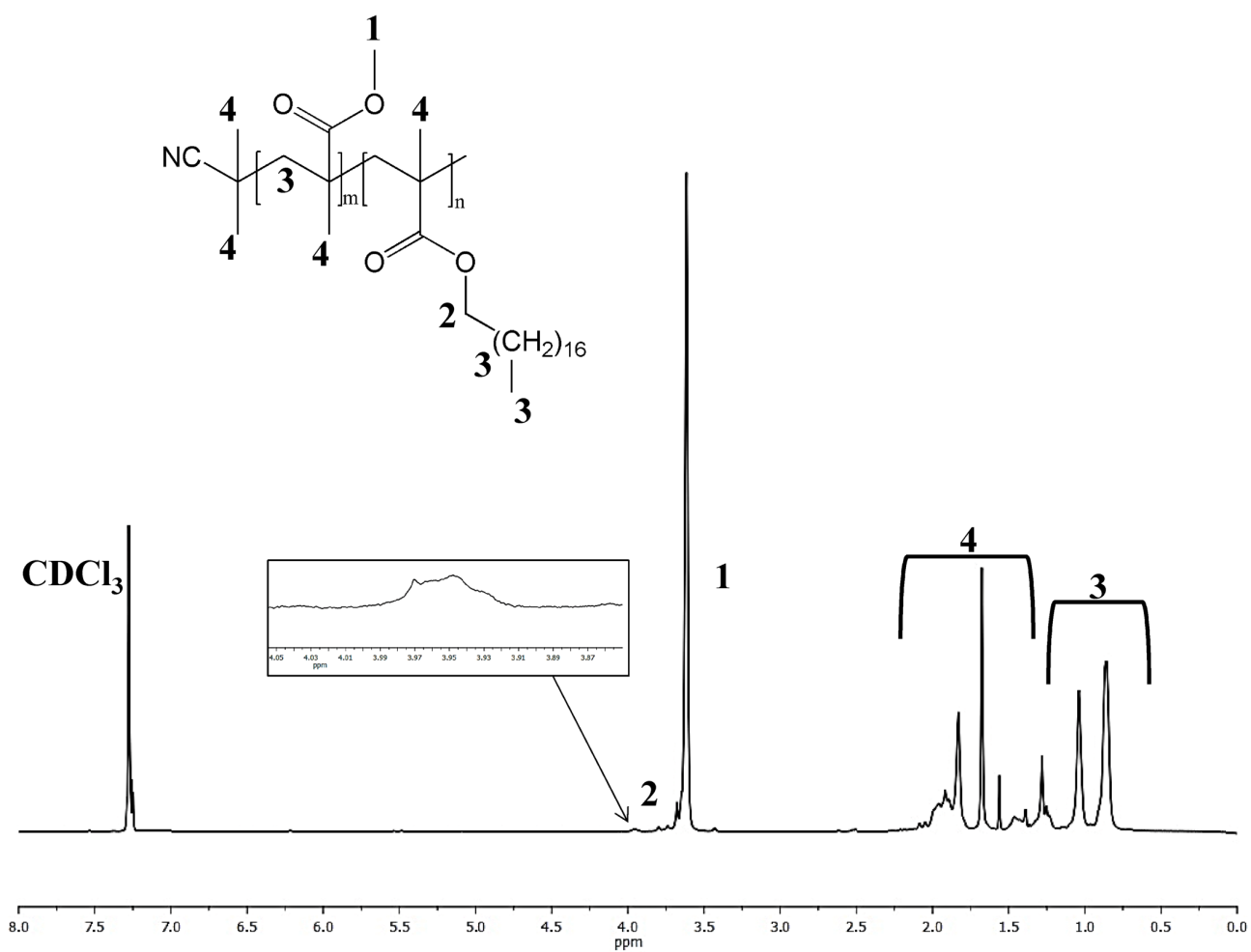
202

203 3. RESULTS and DISCUSSION

204 3.1 Synthesis, characterization and aging study of MMA_STEA copolymers

205 Novel protective polymers (MMA_STEA) were through the free radical polymerization between
206 MMA and STEA, varying the molar percentage of STEA with respect to MMA co-monomer (1.0-
207 2.5-5.0% mol/mol). Their actual chemical structures were determined via ^1H NMR spectroscopy
208 (Figure 2): by comparing the spectra of MMA_STEA samples (Figure 3) with different STEA
209 loadings, the increase of the integral area of the peak relative to STEA (**a**) is clearly appreciable.

210 Furthermore, the real amount of STEA in MMA_STEA copolymers can be quantitatively
211 determined by ^1H NMR spectra using Equation 1 where " I_{STEA} " is the integral area of peak [a],
212 " I_{MMA} " is the integral area of peak [b], "2" corresponds to the number of STEA protons related to
213 the integral area of peak [a] and "3" is the number of MMA protons for the integral area of peak
214 [b].
215



216
217 **Figure 2.** ^1H NMR spectrum of MMA_STEA_1.0.
218

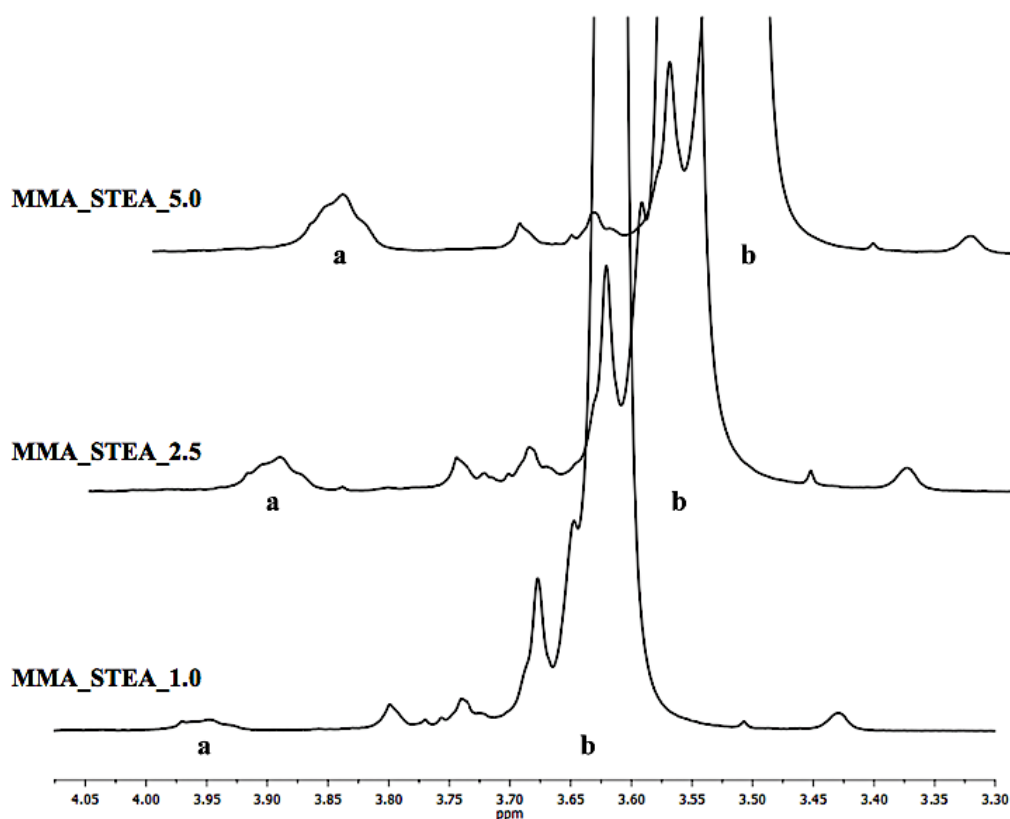


Figure 3. Magnification of MMA_STEAs ¹H NMR spectra.

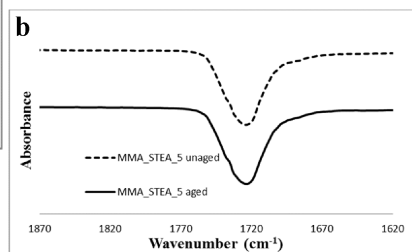
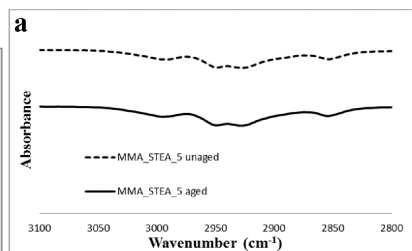
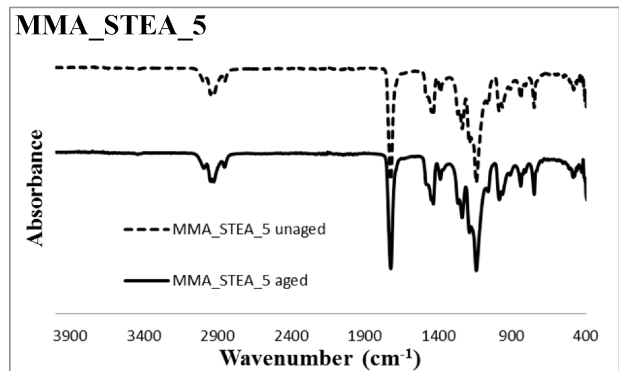
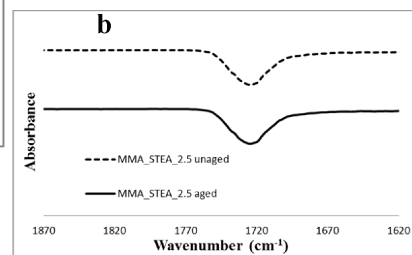
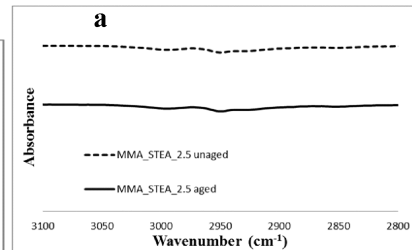
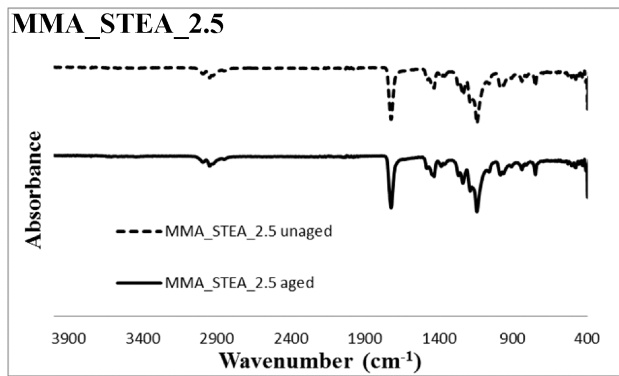
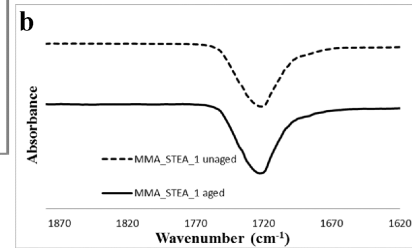
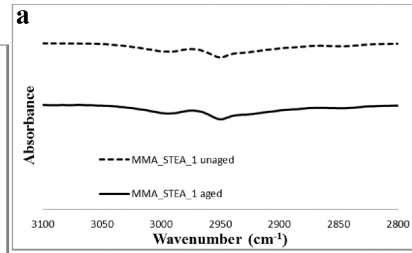
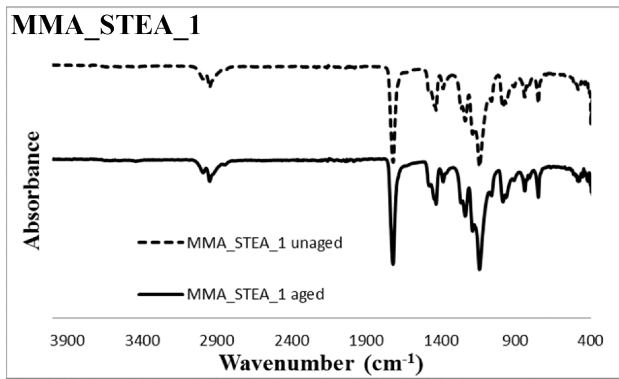
$$\text{STEA \% mol/mol} = \frac{(I_{\text{STEA}}/2)}{(I_{\text{MMA}}/3)} \quad (1)$$

The results are reported in Table 1, highlighting that the theoretical and the experimental values are fully in accordance, confirm that MMA_STEA copolymers were successfully synthesized.

Sample	theoretical STEA % (mol/mol)	real STEA % (mol/mol)
MMA_STEA_1.0	1.0	1.0
MMA_STEA_2.5	2.5	2.1
MMA_STEA_5.0	5.0	5.3

Table 1. STEA molar percentage in MMA_STEAs determined via ¹H NMR spectroscopy.

To determine the long-term stability of the new tailored MMA_STEA resins, a UV accelerated exposure test was performed. Figure 4 shows a comparison between FT-IR spectra of different MMA_STEAs, collected before and after the aging test. The peak (a) in the ~3100–2800 cm⁻¹ range is related to the bending of C-H aliphatic bonds [21]; the stretching of carbonyl ester groups (C=O) (b) lies in the range between ~1750 and 1600 cm⁻¹ [21].



233

234

235

Figure 4. FT-IR spectra of MMA_STEAs collected before and after the aging test, and magnification of a) bending C-H area and b) stretching C=O area.

236 In the case of polyacrylates, the shape of (a) and (b) absorption peaks changes dramatically after the
 237 UV aging test, showing a significant variation of the bands related to C-H aliphatic bonds and the
 238 same carbonyl groups, due to degradation phenomena of polymeric bonds (breaking of
 239 macromolecular chains where aliphatic and carbonyl groups are present) [12]. This behaviour is
 240 probably due to the presence in polymer structures of hydrogen atoms, deriving from acrylic
 241 monomers, in alpha position to carbonyl groups that are able to start the photo-chemical
 242 degradation of the polymers themselves [22]. Here, no significant variations are detectable among
 243 the MMA_STEA FT-IR spectra (Figure 4) collected before and after the aging test, suggesting the
 244 high photochemical stability of the new synthesized resins. Furthermore, the effect of UV exposure
 245 can be highlighted by the evaluation of the number average molecular weight (\overline{Mn}), the weight
 246 average molecular weight (\overline{Mw}), the peak molecular weight (Mp) and the molecular weight
 247 distribution (D) by GPC analyses (Table 2). MMA_STEA_1.0/2.5/5.0 polymers remain soluble in
 248 DCM after the aging test, suggesting the absence of radicals that allow the formation of a partially
 249 reticulated polymer via cross-linking reactions [12]. Furthermore, the variation of the molecular
 250 weights and their relative distribution (Table 2) before and after the aging test is negligible, clearly
 251 evidencing the photo-stability of the tailored resins [23].

252

Sample	\overline{Mn} (Da)	\overline{Mw} (Da)	Mp (Da)	D	T _g (°C)
MMA_STEA_1.0 unaged	4500	12000	10000	3.4	95.3
MMA_STEA_1.0 aged	4400	11900	9800	3.3	97.2
MMA_STEA_2.5 unaged	3800	11000	9300	2.9	75.7
MMA_STEA_2.5 aged	3700	10800	9300	2.8	75.3
MMA_STEA_5.0 unaged	3700	17800	9900	4.8	69.0
MMA_STEA_5.0 aged	3600	17700	9800	4.9	66.2

253 **Table 2.** GPC data and glass transition temperatures of MMA_STEA samples before and after the aging test.

254

255 MMA_STEAs thermal properties were also assessed and compared with the ones obtained after the
 256 UV aging test (Table 3). The glass transition temperatures (T_g) of MMA_STEA_1.0/2.5/5.0 samples
 257 are respectively 95.3, 75.7 and 69.0°C. Thus, by increasing the STEA amount, *i.e.* aliphatic pendant
 258 chains in the final polymer, the T_g tends to decrease. After the aging test, MMA_STEAs T_g remains
 259 almost the same, in according with FT-IR and GPC analyses. The comparison of FT-IR, GPC and
 260 DSC data measured before and after the aging test demonstrates that a polymer resin prepared
 261 starting from MMA and STEA is an efficient way to obtain a protective with enhanced photo

262 chemical durability. Within this context, the use of MMA_STEA based resins can be a way to
263 obtain a satisfactory protective for mortar substrates.

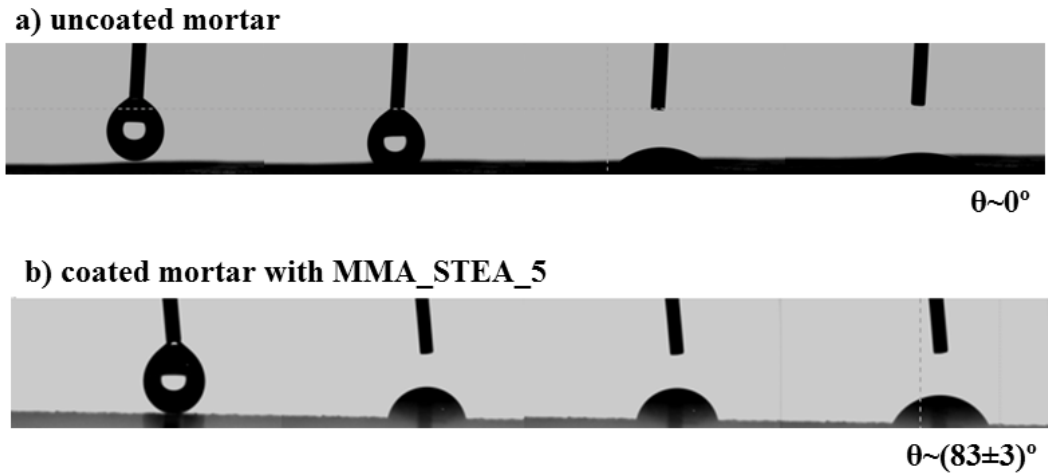
264 **3.2 Deposition of MMA_STEA copolymers onto home-made mortars and relative protective** 265 **features**

266 Both the morphology and the elementary composition of the mortar sample were preventively
267 characterized by SEM-EDX analyses (Figure S1), in order to investigate the efficiency of mortar
268 tiles formation in terms of surface homogeneity and quality of carbonation process. In according to
269 the data reported in literature [24], the mortar appears as a homogeneous surface, without cracks
270 and holes, characterized by an EDX peak related to calcium element having high intensity,
271 confirming the successful carbonation process. Indeed, the pumice presence is reported not only to
272 give mortars excellent binding and durability features, improving both their strength and abrasion
273 resistance, but also to reduce the flow/workability of fresh mortars [24].

274 MMA_STEA_1.0/2.5/5.0 resins were applied via paint-coating onto a mortar substrate prepared as
275 reported in Materials and Methods section, and their wetting properties, CIELab colorimetric
276 features, water absorption by capillarity capability and WVP properties were assessed. Furthermore,
277 all of these analyses were repeated after an UV accelerated aging test. The bare mortar surface
278 shows a high-water wettability, not measurable by contact angle instrument due to the immediate
279 absorption of water onto mortar tile (Figure 5a). When MMA_STEA resins were applied, at first the
280 coatings limit the water absorption onto mortar surface (Figure 5b) allowing the contact angle
281 measurements: actually, WCA values (Table 3, 2nd column) increase at increasing of the STEA
282 loading, passing from 75° in the case of MMA_STEA_1.0 to 83° for MMA_STEA_5.0, almost
283 reaching the hydrophobicity threshold (Figure 5b). The WCAs of coated mortars were re-measured
284 after an UV accelerated aging test and, in according to the data previously presented and discussed,
285 it is possible to observe from Table 3 that the wetting features remain similar.

286

287



288
289

Figure 5. WCA frames of a) uncoated mortar and b) coated mortar with MMA_STEA_5.0.

Sample	θ ($^\circ$)	ΔE
MMA_STEA_1.0 unaged	75 \pm 4	3.1
MMA_STEA_1.0 aged	68 \pm 5	
MMA_STEA_2.5 unaged	79 \pm 3	2.4
MMA_STEA_2.5 aged	73 \pm 3	
MMA_STEA_5.0 unaged	88 \pm 3	0.9
MMA_STEA_5.0 aged	75 \pm 5	

290 **Table 3.** WCA data of MMA_STEA-based mortars before and after the aging test and colorimetric variations between
291 unaged and aged coated mortars.

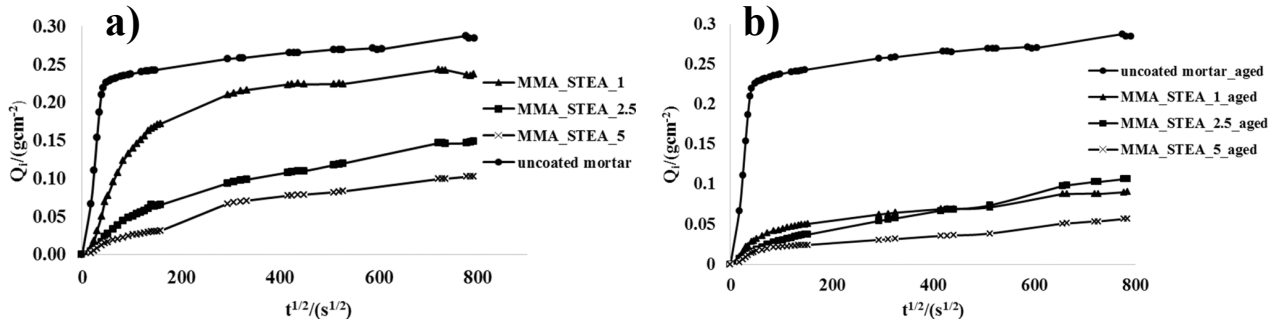
292

293 To corroborate the optical durability of the as prepared polymers, the CIELab color space [25] was
294 determined. It provides a standard and approximately uniform scale that can be used to compare the
295 color modification of an object over the time or after a critical event, such as solar and/or thermal
296 aging tests [26]. In this work, the colorimetric measurements were carried out on the MMA_STEA-
297 based mortars treated before and after the UV aging test to determine if chromatic alterations occur
298 after the prolonged exposition to an ultraviolet radiation. According to the literature [18], a
299 chromatic difference, expressed by the ΔE parameter, less than or equal to 5 ($\Delta E \leq 5$) is not
300 considered significant. ΔE values for MMA_STEAs, shown in Table 3 (3rd column), were
301 calculated from DRS analyses. For all the samples, the undesired threshold was not achieved, thus
302 the chromatic alteration can be considered negligible. The unchanged optical properties of the novel
303 resins confirm the durability results obtained via FT-IR, GPC and DSC analyses; MMA_STEAs
304 seem to be promising as mortar protective coatings.

305 Then, the water absorption test by capillarity is one of the most effective methods to evaluate the
306 penetration and the relative capillarity rise of water within a mineral substrate such mortars, and to
307 estimate the effectiveness of a water-repellent treatment. In this work, the measures of water

308 absorption by capillarity on bare and coated mortars were conducted in accordance with UNI 10859
 309 standard method. Furthermore, the total amount of water absorbed by the material (Q_f), the capillary
 310 absorption (CA), the relative capillarity index (CI_{rel}) were determined, accordingly. Figure 5 shows
 311 the results of bare and MMA_STEA-based mortars, both before (Figure 6a) and after the UV aging
 312 test (Figure 6b).

313



314

315 **Figure 6.** Capillarity data for bare mortar and mortars coated with MMA_STEA samples measured a) before and b)
 316 after the aging test.

317

318 A different trend between the water absorption curves of the uncoated and coated mortars can be
 319 clearly observed. The capillarity curve of the untreated mortar is characterized by a very steep linear
 320 step followed by a plateau region. This behavior corresponds to the saturation of the material
 321 occurred after a fast absorption of water (saturation time: 3 hours). On the contrary, MMA_STEA-
 322 based samples do not reach saturation and there is a gradual increase of the water absorbed as a
 323 function of time. Indeed, the mortar water absorption is reduced by the presence of the protective
 324 coatings, which waterproof the mortars surface, preventing the rising of water. Furthermore, the
 325 waterproofing behavior of MMA_STEA resins increases as the amount of STEA gets higher. As
 326 reported in Table 4, the total amount of water absorbed by the material (Q_f parameter) decreases as
 327 the loading of STEA in MMA-based copolymers increases, as well as CA and CI_{rel} parameters.

328

Sample	Q_f ($g \times cm^{-2}$)	$CA \times 10^3$ ($g \times cm^{-2} \times t^{1/2}$)	IC_{rel}	RVP (%)
bare mortar-unaged	0.28	5.50	-	-
bare mortar-aged	0.28	5.47	-	-
MMA_STEA_1.0-unaged	0.24	1.70	0.72	41
MMA_STEA_1.0-aged	0.09	0.67	0.23	5
MMA_STEA_2.5-unaged	0.60	0.60	0.36	34
MMA_STEA_2.5-aged	0.11	0.04	0.23	32

MMA_STEA_5.0-unaged	0.40	0.40	0.24	63
MMA_STEA_5.0-aged	0.06	0.05	0.13	41

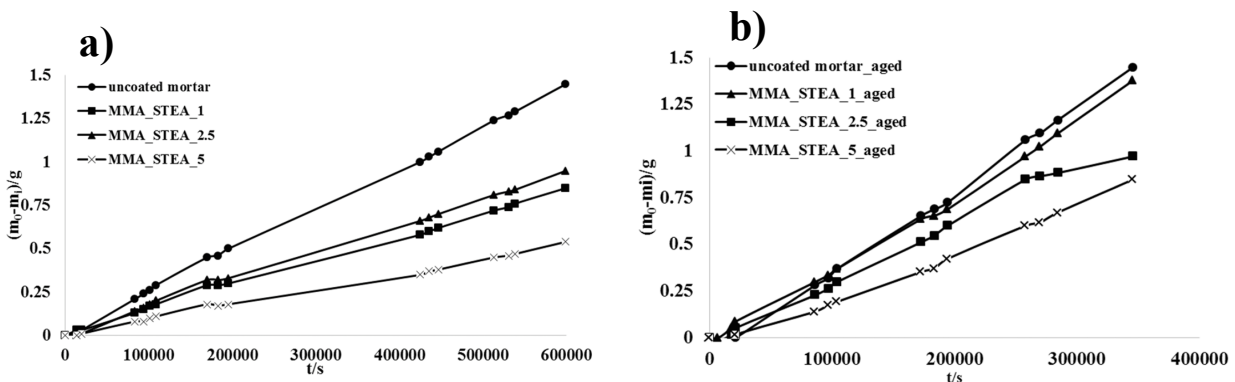
Table 4. Capillarity and permeability parameters for bare mortar and MMA_STEA-based mortars.

329
330

331 The capillarity tests repeated on the aged samples (Figure 6b) show that there is an increase of the
332 waterproofing behavior of the synthesized resins and consequently, a decrease of Q_f , CA and IC_{rel}
333 parameters, in accordance with the high photochemical stability of MMA_STEA coatings (Table 4).
334 The improvement of capillarity performances for aged MMA_STEAs mortars in comparison to
335 unaged samples, is probably due to the complete evaporation of the paint-coating solvent traces
336 [27,28].

337 Ideally, a protective coating for a mortar should prevent the capillary absorption of water, but at the
338 same time, it should allow the permeation of water vapour through the material pores. Indeed, a
339 hard reduction of WVP can damage the mortar, since a long permanence of water and aqueous
340 solutions inside the porous matrix of the mineral can favour the formation of salt aggregates able to
341 determine mechanical stress such as cracks, promoting the detachment of the protective coating
342 from the mortars surface [29,30]. Indeed, the parameter related to the reduction of water vapour
343 permeability (RVP) was determined for either the unaged or aged coated mortars. According to the
344 standard protocol, a polymer material cannot be used as protective for mortar substrate if $RVP >$
345 50%. Figure 7a and b show the WVP curves of unaged and aged MMA_STEA-based mortars,
346 respectively. Comparing WVP data, in the case of unaged samples (Figure 7a and Table 4, 6th
347 column), it is possible to observe a reduction of permeability for all the STEA-clad mortars.
348 Specifically, MMA_STEA_5.0 reaches an RVP value of 63%, out of the permitted threshold.

349
350



351
352

Figure 7. Permeability data for bare mortar and mortars coated with MMA_STEA samples measured a) before and b) after the aging test.

353
354
355

356 In the case of aged samples (Figure 7b), there is an improved permeability for all the coated
357 mortars, *i.e.* all the coated-samples with RVP data always <50%. Furthermore, as for unaged
358 samples, the permeability gets higher as STEA amount increases. As stated for capillarity tests, the
359 increase of permeability performances for aged MMA_STEAs mortars in comparison to unaged
360 ones is probably due to the complete evaporation during the aging test of the paint-coating solvent
361 traces that could have remained inside the polymer coatings. In the future, best conditions of
362 coating application and drying, in terms of resin deposition technique and the nature of the solvent,
363 will be studied. Moreover, by correlating MMA_STEAs chemical data obtained before and after the
364 aging test, the novel polymer coatings prepared in this work could be, in a future, used as innovative
365 waterproofing and durable protective also for several types of mortar.

366

367 4. CONCLUSIONS

368 The development of new polymer coatings characterized by hydrophobic properties and high photo-
369 chemical stability is the key of success in the field of building materials protection for cultural
370 heritage and modern architecture. Within this context, the use of polymer resins bearing methacrylic
371 and stearyl monomers along the polymeric chain can be a way to create tailor-made waterproofing
372 materials with enhanced UV durability.

373 A new kind of polymer protective was prepared via free radical polymerization between methyl
374 methacrylate (MMA) and stearyl methacrylate (STEA) comonomers, varying the molar percentage
375 of STEA with respect to MMA (1.0-2.5-5.0% mol/mol). In order to determine the long-term
376 properties of MMA_STEA resins, an accelerated UV exposure test was performed. The
377 macromolecular structure, molecular weights and thermal features of MMA_STEAs were
378 investigated before and after an UV test via ¹H NMR and Fourier Transform-Infrared (FT-IR)
379 spectroscopies, Gel Permeation Chromatography (GPC) and Differential Scanning Calorimetry
380 (DSC) studies.

381 Combining the data measured before and after the aging test, it was possible to conclude that a
382 polymer protective prepared starting from methyl and stearyl methacrylates monomers is an
383 efficient way to obtain a resin with satisfactory photo-chemical stability.

384 Furthermore, MMA_STEA resins were successfully applied onto air-hardening calcic lime mortar
385 tiles and their wetting properties, CIELab colorimetric features, capillarity and permeability were
386 assessed and compared before and after the UV aging test. It was found that all the new resins
387 synthesized maintain unchanged their features in terms of waterproofing resins with high durability
388 and capability to favor the water vapor transpiration and to avoid the water absorption inside the
389 mineral substrate over the time.

390 To the authors' best knowledge, the present results, *i.e.* the development of durable waterproofing
391 resins-based on MMA_STEA polymers, have never been reported in previous scientific works.
392 The work will be continued with an emphasis placed on the study of the influence of different
393 processing conditions, such as the loading of STEA monomer, on the properties of MMA_STEA
394 resin. Water repellent behavior, chemical and biological durability will be investigated further on.

395

396 **Acknowledgments**

397 This research did not receive any specific grant from funding agencies in the public, commercial, or
398 not-for-profit sectors. The authors gratefully acknowledge Maurizio Fogazzi (ChemArt) for his
399 precious advice concerning the mortars formulation.

400

401 **Supporting Information**

402 Figure S1: SEM-EDX analyses data relative to bare mortars.

403

404 **REFERENCES**

- 405 [1] C. Esposito Corcione, N. De Simone, M.L. Santarelli, M. Frigione, Protective properties and
406 durability characteristics of experimental and commercial organic coatings for the
407 preservation of porous stone, *Prog. Org. Coatings*. 103 (2017) 193–203.
408 doi:10.1016/j.porgcoat.2016.10.037.
- 409 [2] E. Capezzuoli, A. Gandin, M. Pedley, Decoding tufa and travertine (fresh water carbonates)
410 in the sedimentary record: The state of the art, *Sedimentology*. 61 (2014) 1–21.
411 doi:10.1111/sed.12075.
- 412 [3] Y.-W. Wang, Y.-Y. Kim, C.J. Stephens, F.C. Meldrum, H.K. Christenson, In Situ Study of
413 the Precipitation and Crystallization of Amorphous Calcium Carbonate (ACC), *Cryst.*
414 *Growth Des.* 12 (2012) 1212–1217. doi:10.1021/cg201204s.
- 415 [4] G. Cappelletti, P. Fermo, M. Camiloni, Smart hybrid coatings for natural stones
416 conservation, *Prog. Org. Coatings*. 78 (2015) 511–516. doi:10.1016/j.porgcoat.2014.05.029.
- 417 [5] P. Fermo, G. Cappelletti, N. Cozzi, G. Padeletti, S. Kaciulis, M. Brucale, M. Merlini,
418 Hydrophobizing coatings for cultural heritage. A detailed study of resin/stone surface
419 interaction, *Appl. Phys. A*. 116 (2014) 341–348. doi:10.1007/s00339-013-8127-z.
- 420 [6] C. Forrest, *International law and the protection of cultural heritage*, Routledge, 2012.
- 421 [7] D. Michoinovà, *New materials for the protection of cultural heritage*, 2007.
- 422 [8] M. Cocca, L. D'Arienzo, L. D'Orazio, G. Gentile, E. Martuscelli, Polyacrylates for
423 conservation: Chemico-physical properties and durability of different commercial products,

- 424 Polym. Test. 23 (2004) 333–342. doi:10.1016/S0142-9418(03)00105-3.
- 425 [9] O. Cocco, M. Carboni, G. Carcangiu, P. Meloni, A. Murru, F. Persia, L. Solla, Crime art on
426 the stone: Graffiti Vandalism on cultural heritage and the anti-graffiti role in its surfaces
427 protection, *Period. Di Mineral.* 84 (2015) 435–452. doi:10.2451/2015PM0023.
- 428 [10] F. Cappitelli, C. Sorlini, Microorganisms attack synthetic polymers in items representing our
429 cultural heritage, *Appl. Environ. Microbiol.* 74 (2008) 564–569. doi:10.1128/AEM.01768-
430 07.
- 431 [11] L. Toniolo, T. Poli, V. Castelvetro, A. Manariti, O. Chiantore, M. Lazzari, Tailoring new
432 fluorinated acrylic copolymers as protective coatings for marble, *J. Cult. Herit.* 3 (2002) 309–
433 316. doi:10.1016/S1296-2074(02)01240-2.
- 434 [12] O. Chiantore, M. Lazzari, Photo-oxidative stability of paraloid acrylic protective polymers,
435 *Polymer (Guildf).* 42 (2001) 17–27. doi:10.1016/S0032-3861(00)00327-X.
- 436 [13] V. Sabatini, C. Cattò, G. Cappelletti, F. Cappitelli, S. Antenucci, H. Farina, M.A. Ortenzi, S.
437 Camazzola, G. Di Silvestro, Protective features, durability and biodegradation study of acrylic
438 and methacrylic fluorinated polymer coatings for marble protection, *Prog. Org. Coatings.* 114
439 (2018). doi:10.1016/j.porgcoat.2017.10.003.
- 440 [14] V. Sabatini, H. Farina, A. Montarsolo, E. Pargoletti, M.A. Ortenzi, G. Cappelletti,
441 Fluorinated polyacrylic resins for the protection of cultural heritages: The effect of fluorine
442 on hydrophobic properties and photochemical stability, *Chem. Lett.* 47 (2018).
443 doi:10.1246/cl.171020.
- 444 [15] G. Alessandrini, M. Aglietto, V. Castelvetro, F. Ciardelli, R. Peruzzi, L. Toniolo,
445 Comparative evaluation of fluorinated and unfluorinated acrylic copolymers as water-
446 repellent coating materials for stone, *J. Appl. Polym. Sci.* 76 (2000) 962–977.
447 doi:10.1002/(SICI)1097-4628.
- 448 [16] UNI 10925:2001, Beni culturali - Materiali lapidei naturali ed artificiali - Metodologia per l
449 irraggiamento con luce solare artificiale.
- 450 [17] G. Cappelletti, P. Fermo, F. Pino, E. Pargoletti, E. Pecchioni, F. Fratini, S.A. Ruffolo, M.F.
451 La Russa, On the role of hydrophobic Si-based protective coatings in limiting mortar
452 deterioration, *Environ. Sci. Pollut. Res.* 22 (2015) 17733–17743. doi:10.1007/s11356-015-
453 4962-0.
- 454 [18] M.F. La Russa, S. a. Ruffolo, N. Rovella, C.M. Belfiore, A.M. Palermo, M.T. Guzzi, G.M.
455 Crisci, Multifunctional TiO₂ coatings for Cultural Heritage, *Prog. Org. Coatings.* 74 (2012)
456 186–191. doi:10.1016/j.porgcoat.2011.12.008.
- 457 [19] 15801 UNI EN, Conservation of cultural property - Test methods - Determination of water

- 458 absorption by capillarity, (2010).
- 459 [20] 15803 UNI EN, Conservation of cultural property - Test methods - Determination of water
460 vapour permeability, (2009).
- 461 [21] W. Huang, J.-B. Kim, M.L. Bruening, G.L. Baker, Functionalization of Surfaces by Water-
462 Accelerated Atom-Transfer Radical Polymerization of Hydroxyethyl Methacrylate and
463 Subsequent Derivatization, *Macromolecules*. 35 (2002) 1175–1179. doi:10.1021/ma011159e.
- 464 [22] I.C. McNeill, S.M.T. Sadeghi, Thermal stability and degradation mechanisms of poly(acrylic
465 acid) and its salts: Part 1 - Poly(acrylic acid), *Polym. Degrad. Stab.* 29 (1990) 233–246.
466 doi:10.1016/0141-3910(90)90034-5.
- 467 [23] P. Cowley, E.J. Ronald, H.W. Melville, The photo-degradation of polymethylmethacrylate,
468 *Proc. R. Soc. Lond. A.* 210 (1952) 461–481.
- 469 [24] O. Karahan, K.M.A. Hossain, C.D. Atis, M. Lachemi, E. Ozbay, Ground Granulated Pumice-
470 Based Cement Mortars Exposed to Abrasion and Fire, *Arab. J. Sci. Eng.* 42 (2017) 1321–
471 1326. doi:10.1007/s13369-016-2403-0.
- 472 [25] K. McLaren, XIII-The development of the CIE 1976 ($L^* a^* b^*$) uniform colour space and
473 colour-difference formula, *J. Soc. Dye. Colour.* 92 (1976) 338–341.
- 474 [26] C. Connolly, T. Fleiss, A study of efficiency and accuracy in the transformation from RGB
475 to CIELab color space, *IEEE Trans. Image Process.* 6 (1997) 1046–1048.
- 476 [27] S. Sen, Equivalence between polymer nanocomposites and thin polymer films: Effect of
477 processing conditions and molecular origins of observed behavior, *Eur. Phys. J. Spec. Top.*
478 141 (2007) 161–165.
- 479 [28] L. Chang, Effect of trace solvent on the morphology of P3HT: PCBM bulk heterojunction
480 solar cells, *Adv. Funct. Mater.* 21 (2011) 1779–1787.
- 481 [29] M. Do Rosario Veiga, Lime-based mortars: viability for use as substitution renders in
482 historical buildings, *Int. J. Architectural Herit.* 4 (2010) 177–195.
- 483 [30] S.K. D., R. Hooton, M.D.A. Thomas, Testing the chloride penetration resistance of concrete:
484 a literature review.